RF/Microwave Characterization of Multilayer Ceramic-Based MCM Technology

Albert Sutono, Anh-Vu H. Pham, *Member, IEEE,* Joy Laskar, and William R. Smith

***Abstract*—We present RF/microwave characterization of a 20-layer ceramic-based multichip module (MCM-C) on low temperature co-fired ceramic (LTCC). We investigated material properties and performance of embedded passives by design, fabrication and characterization of planar and multilayer integral inductors. Uniform dielectric constant, low loss property and high Q passives fabricated using this technology demonstrate the feasibility for implementing hybrid RF/microwave systems.**

***Index Terms*—Embedded passives, multi-layer, RF/microwave, 3-D inductors.**

I. Introduction

MULTILAYER multichip modules (MCM's) offer the potential for compact, high performance and high functionality implementation in RF/Microwave packaging applications. Low temperature co-fired ceramic (LTCC)-based MCM-C is capable of embedding passives as well as implementing dense interconnects [1]–[3]. Passive components occupy a significant fraction of the total area in monolithic microwave integrated circuits (MMIC's). It is desirable to reduce the area occupied by the MMIC and achieve better performance by implementing passive elements on MCM [4], [5]. In this paper, we extract frequency dependent dielectric and loss properties of LTCC to 10 GHz. In addition, we design, characterize and develop circuit models for multilayer (3-D) spiral inductors for the first time as well as planar spiral inductors. The 2-D planar inductors exhibit an improved Q-factor and effective inductance compared to the previously reported work [5].

The LTCC process offers screen printing and low-loss stacked via processes as well as high conductivity metallization useful for high frequency applications [1]. The substrate material for the 20-layer LTCC is 951-AT ceramic (a trade mark of Dupont) and each layer is 3.6 mils thick. The metallization of the buried layer is 7 μm silver alloy and the surface metallization can be 9 μm silver or palladium alloy or 7 μm wire bondable gold. Fig. 1 shows the actual top view and cross sectional schematic diagram of the 20 layer LTCC test coupon including the layer designation.

Manuscript received January 10, 1999; revised May 10, 1999. This paper was presented at the Seventh Topical Meeting on Electrical Performance of Electronic Packaging, United States Military Academy, West Point, NY, October 26–28, 1998. This work was supported in part by the NSF Packaging Research Center, Georgia Institute of Technology under Contract ECE-9 402 723 and NSF Career Award ECS-9 623 964, and National Semiconductor's LTCC Fabrication Facility.

A. Sutono and J. Laskar are with the Packaging Research Center, School of Electrical and Computer Engineering, Georgia Institute of Technology, Atlanta, GA 30332-0250 USA.

A.-V. H. Pham is with the Department of Electrical and Computer Engineering, Clemson University, Clemson, SC 29634-0915 USA.

W. R. Smith is with the National Semiconductor Corporation, Newport Beach, CA 92663 USA.

Publisher Item Identifier S 1521-3323(99)06574-0.

The initial processing step involves material preparation by mixing the ceramic powder with organic binders that allow fabrication into a flat tape. This flat tape mixture is then sliced and dried to become a 3.6 mils thick thin film. This thin piece of tape, called unfired tape, can be rolled up when not in use and unreeled when it is going to be processed. The first processing step is drilling holes on the unfired tape at the locations that contain vias followed by printing metallization. For multilayer construction, the layers of tape are placed on top of each other, and the hole drilling and metallization printing processes are repeated for each layer. Once all vias have been formed and every layer has been screen patterned with metallization, the stacked tape is pressed together and heated (fired) at approximately 875 °C so that the layers become a monolithic slab. Unlike High Temperature Co-fired Ceramic (HTCC), LTCC process allows the use of high conductivity metals such as silver and gold since the melting point of these metal is well *above* the temperature at which the LTCC stack is fired. In HTCC process, the stacked tape is fired at a much higher temperature requiring the use of metallization having an even higher melting point. Tungsten, typically used for HTCC process, has less than half the conductivity than silver and gold used in LTCC process.

II. Experiments

A. Material Characterization

The relative permittivity ε_r as a function of frequency is an important design parameter and typically only given at low frequencies by the manufacturer. We apply a thru-reflect-line (TRL) calibration [6] using HP8510C network analyzer and air coplanar microprobes on a set of coplanar waveguide (CPW) calibration standards with 26.6 mils wide center conductor separated by two 40 mils wide ground planes by 8 mil gap to measure the propagation constant γ to 10 GHz [7]–[8]. Fig. 2 shows the coplanar waveguide TRL calibration standards used in material characterization that cover frequency range from 800 MHz to 10 GHz. The effective permittivity is given in terms of γ by $\varepsilon_{\text{eff}} = (c\beta/\omega)^2$ where ω is the angular frequency. The relative permittivity ε_r is computed from ε_{eff} for the CPW using quasi-TEM closed form equations [9]. The uniformity of frequency dependent dielectric constant verified to 10 GHz and typical loss per unit length of a 50 Ω

1521–3323/99$10.00 © 1999 IEEE

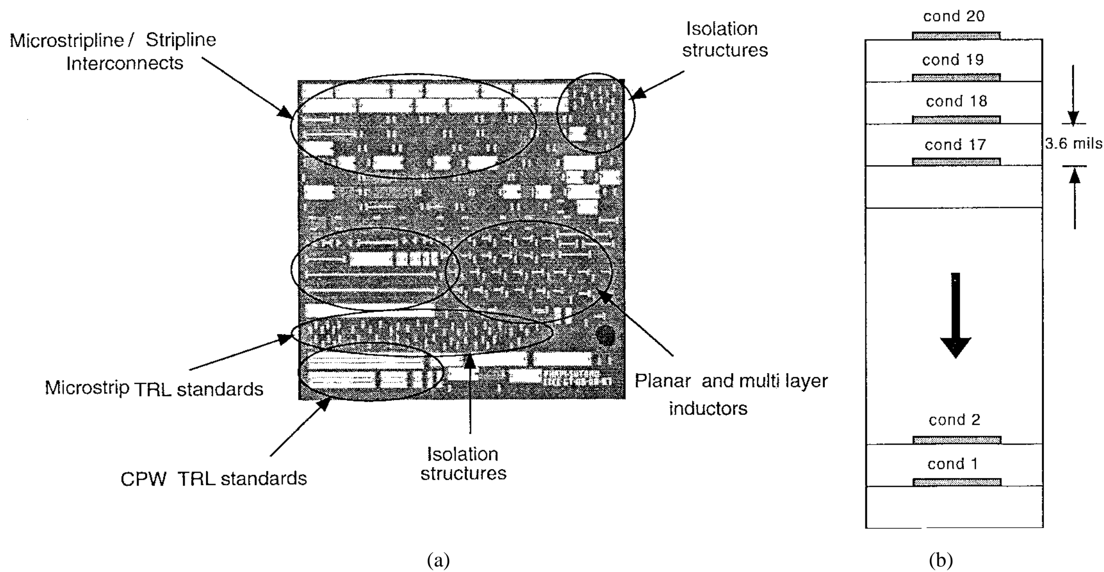

Fig. 1. (a) Top view photographs of a 20 layer LTCC test coupon showing various test structures for material, isolation, interconnects and embedded passive characterization. (b) Cross-sectional view of a 20 layer LTCC substrate indicating layer designation. Each tape layer is 3.6 mils thick.

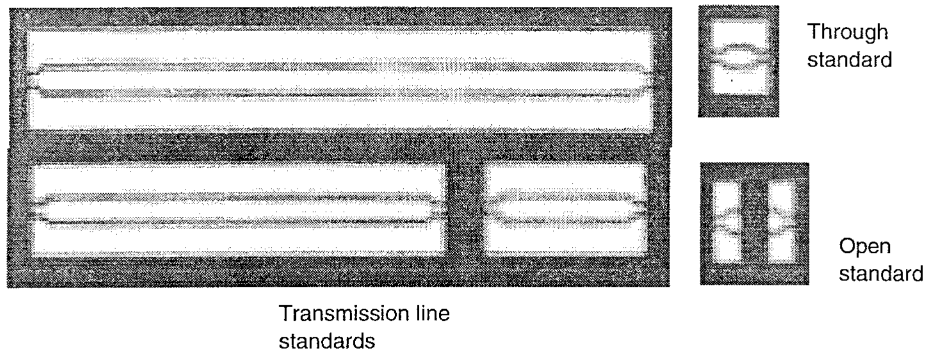

Fig. 2. Coplanar waveguide TRL calibration standards fabricated to extract dielectric constant and loss properties of LTCC material.

transmission lines which includes conductor and dielectric loss are shown in Fig. 3. Both the extracted dielectric constant with nominal value of 7.8 and loss per unit length of 0.18 dB/cm at 10 GHz are consistent with the previously published data [10] which shows a nominal dielectric constant of 7.8 and loss per unit length of 0.14 dB/cm at 10 GHz.

B. Embedded Inductors

The inductor is one of the key components that determines the performance of every RF/microwave circuit, particularly in voltage control oscillator (VCO) [11], power amplifier [12], low noise amplifier and filter. Therefore, the design and use of compact and high Q inductors with the desired inductance is critical to ensure successful circuit operation. The three figure of merits used to evaluate the inductor performance are the quality (Q) factor, the effective inductance (L_{eff}) and the self resonant frequency (SRF). The Q factor of an inductor is a measure of the amount of energy stored compared to the energy loss [9] measured by taking the ratio of the imaginary part to the real part of the input impedance of the inductor obtained from a one-port S-parameter measurement. The effective inductance L_{eff} is the total inductance seen at the input port of the inductor and is obtained by taking the

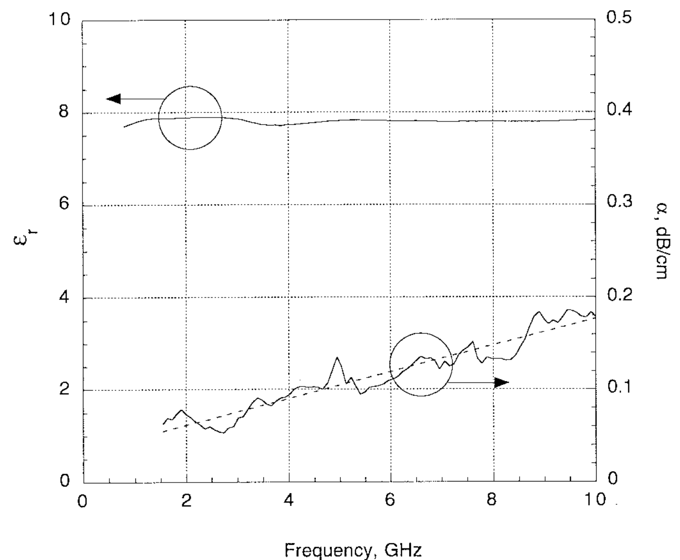

Fig. 3. Measured frequency dependent relative permittivity ε_r and total loss of LTCC extracted using TRL calibration.

ratio of the imaginary part of the input impedance to the angular frequency ω. The angular frequency ω is given by $2\pi f$

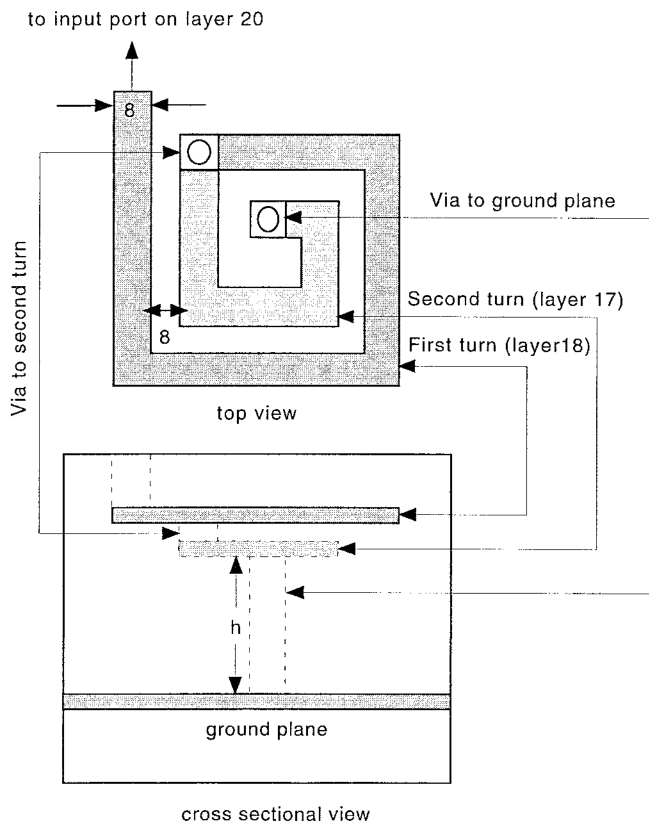

Fig. 4. Top and cross sectional schematic diagram of a multilayer inductor with 8 mil turn width and 1 mil gap between turns.

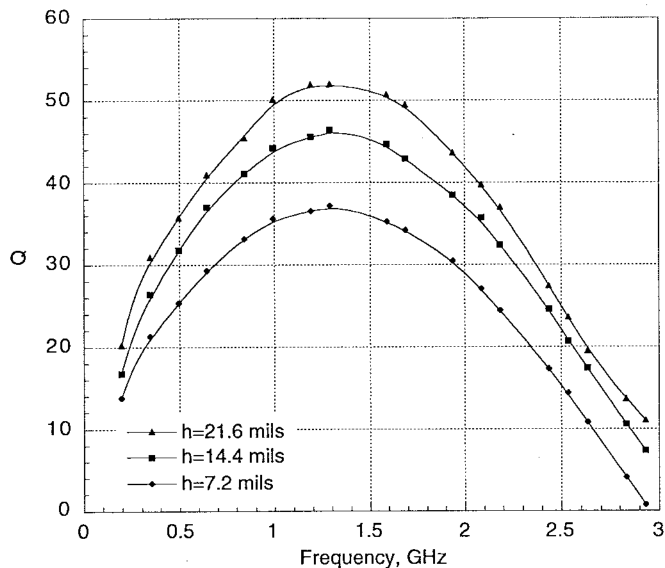

Fig. 5. Measured Q factor of a 2 turn, planar spiral inductors as a function of distance above the ground plane (h).

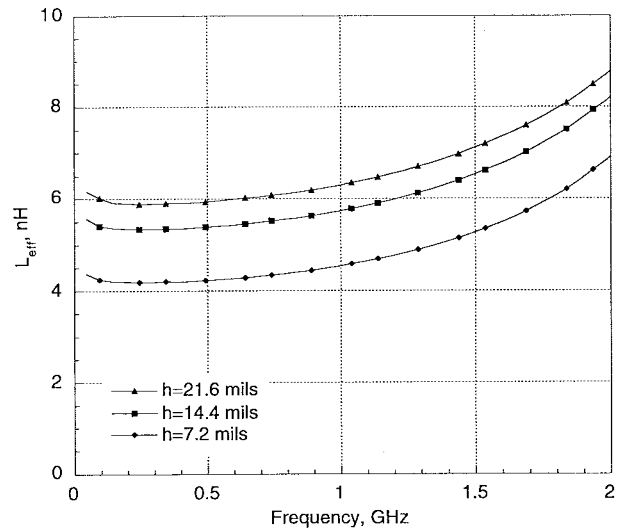

Fig. 6. Measured effective inductance of a 2 turn, planar spiral inductors as a function of distance above the ground plane (h).

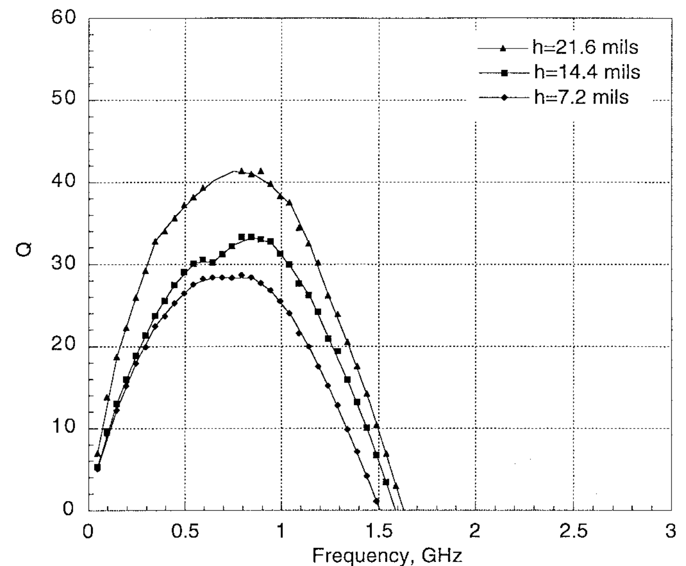

Fig. 7. Measured Q factor of a 3 turn, planar spiral inductors as a function of distance above the ground plane (h).

where f is the frequency. The Self Resonant Frequency (SRF) is the transition frequency point where the input impedance of the inductor changes from inductive to capacitive due to the presence of parasitic elements. It determines the usable frequency range of the inductor. The inductor Q factor depends on several aspects that contribute directly to the distributed loss mechanism including the length (number of turns), line width, turn shape, parasitic capacitance, metallization thickness and conductivity as well as substrate conductivity and dielectric constant. The parasitic capacitance degrades the Q factor because it partially cancels the actual inductance, and therefore reduces the energy storage capability of the inductor while on the other hand, the energy loss per cycle remains constant. The SRF is limited by the inherent existence of distributed parasitic capacitive coupling that occur among the turns of the inductors as well as substrate capacitance which is the capacitance between the inductor turns and the ground plane. Both coupling and substrate capacitance depend on the dielectric constant of the substrate and the number of turns. The coupling capacitance particularly depends on the gap between turns while the substrate capacitance particularly depends on the inductor turn width and the number of turns.

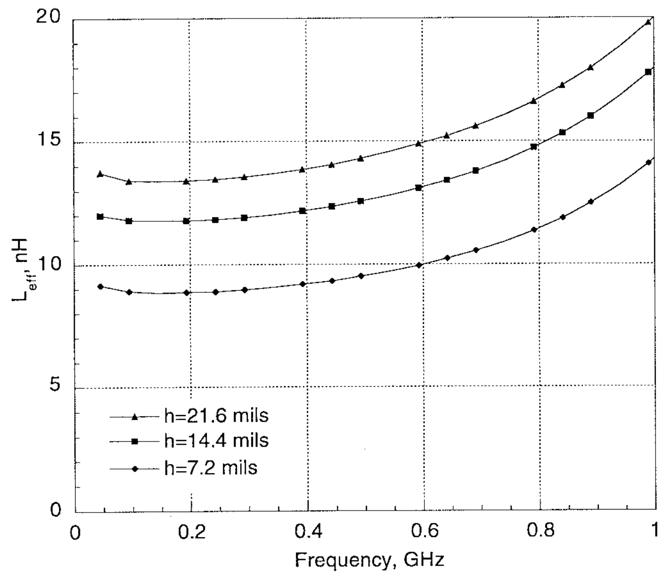

Fig. 8. Measured effective inductance of a 3 turn, planar spiral inductors as a function of distance above the ground plane (h).

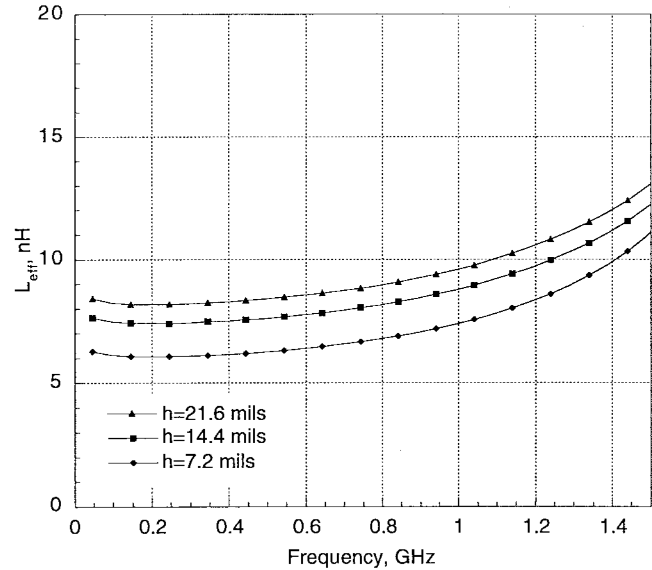

Fig. 10. Measured effective inductance of a 2 turn, 3-D spiral inductors as a function of distance above the ground plane h.

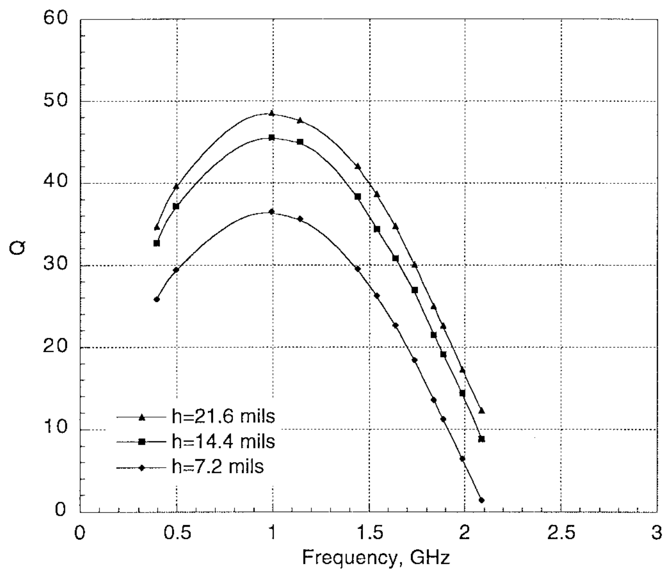

Fig. 9. Measured Q factor of a 2 turn, 3-D spiral inductors as a function of distance above the ground plane h.

TABLE I
SUMMARY OF MEASURED LTCC INDUCTOR PERFORMANCE

Type	# of turns	H (mils)	Q max	SRF (GHz)	L(nH)
2D	2	7.2	37 at 1.3 GHz	2.9	4.8 at 1.3 GHz
2D	2	14.4	47 at 1.3 GHz	3.2	6.1 at 1.3 GHz
2D	2	21.6	52 at 1.3 GHz	3.25	6.7 at 1.3 GHz
2D	3	7.2	28 at 0.8 GHz	1.5	11.4 at 0.8 GHz
2D	3	14.4	34 at 0.8 GHz	1.6	14.7 at 0.8 GHz
2D	3	21.6	41 at 0.8 GHz	1.65	16.6 at 0.8 GHz
3D	2	7.2	36 at 1 GHz	2.1	7.6 at 1 GHz
3D	2	14.4	46 at 1 GHz	2.2	8.9 at 1 GHz
3D	2	21.6	48 at 1 GHz	2.25	9.8 at 1 GHz

Buried inductors are of particular interest since they save a lot of area in the circuit real estate [2], particularly in the 3-D configuration where the inductor turns are expanded vertically not horizontally as in the planar spiral case. We design one-layer buried planar spiral and 3-D inductors in a one-port microstrip configuration [13]. The planar inductors were designed with 2 and 3 turns on layer 19 while the 3-D type is designed with two turns on layer 17 and 18. Each configuration is designed with 8 mil turn width (w), 8 and 1 mil horizontal gap (s) for planar and 3-D types, respectively, and three different distances to the ground plane (h); two layers (7.2 mils), four layers (14.4 mils) and six layers (21.6 mils) as shown in the top and cross-sectional view in Fig. 4. A two-turn planar spiral inductor separated six layers (21.6 mils) above the ground plane can realize a relatively high Q of 52 at 1.3 GHz with an L_{eff} of 6.7 nH as shown in the experimental results in Figs. 5 and 6, respectively. Both L_{eff} and Q can be potentially increased further if the substrate capacitance is reduced by increasing the height from the ground plane. This is a better alternative to realize a higher inductance than by increasing the number of turns which typically causes significant degradation in both Q and SRF as well as significant increase in the area occupied by the inductor. While L_{eff} is more than doubled for a 3 turn as compared to 2 turn planar spiral type as shown in Fig. 8, considerable reduction of Q and SRF caused by increasing number of turn is evident from Fig. 7 in addition to more than twice as much area occupied. The 3-D inductor configuration offers another alternative to obtain more inductance by the presence of more mutual inductive coupling between the turns compared to that of the planar type while maintaining small occupied area. The 2 turn 3-D type inductors yield 2.8 nH more inductance than the 2 turn planar type for 2 and 4 layer gap above the ground plane as shown in Fig. 10. The loss due to via discontinuity [14] causes reduction in Q of 8% or better while increased coupling capacitance between turns causes lower SRF by 31% or better for all 3 different heights above the ground plane in the 3-D configuration as shown in

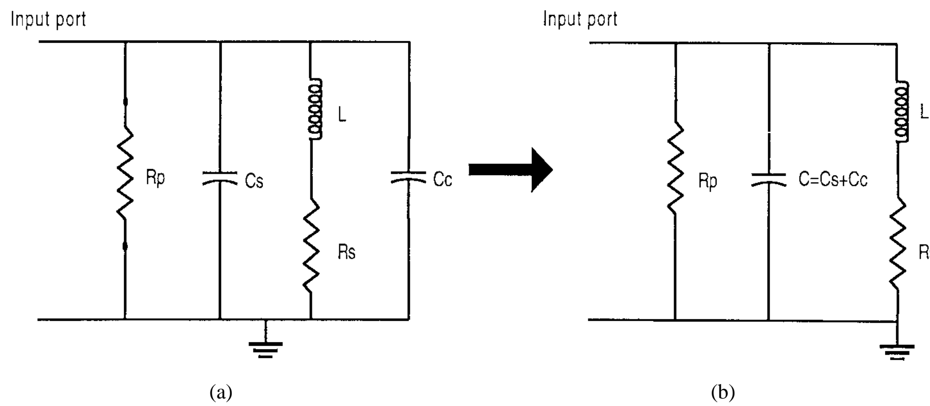

Fig. 11. Complete lumped element circuit model for LTCC inductor (a) and simplified model (b) where the two shunt capacitors C_s and C_c are combined into C.

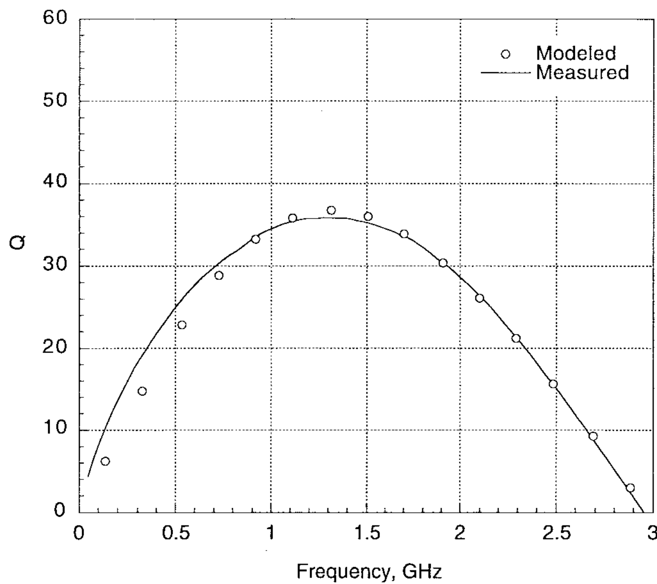

Fig. 12. Measured and modeled Q factor of a 2 turn planar spiral inductor with 2 layer (7.2 mils) distance above the ground plane.

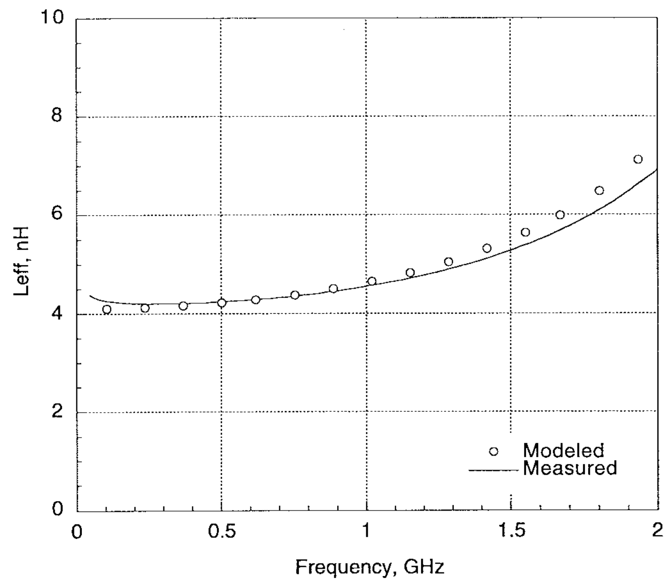

Fig. 13. Measured and modeled effective inductance of a 2 turn planar spiral inductor with 2 layer (7.2 mils) distance above the ground plane.

Figs. 9 and 10, respectively. Table I summarizes the measured performance of LTCC inductors in terms of their maximum Q, SRF and L_{eff} at frequency of maximum Q.

Fig. 11(a) shows the lumped element electrical model of a one port inductor. The model consists of an ideal inductor L in series with a resistor R_s to account for the ideal inductor without any of the parasitic elements and the conductor as well as via loss, respectively. The finite conductivity of the LTCC substrate, the substrate capacitance and coupling capacitance between turns are represented by $R_p, C_,$s and C_c, respectively. Since C_s and C_c are in parallel, the two can be combined together into C. The simplified inductor model is shown in Fig. 11(b). The proposed inductor model shows an excellent correlation to the measured results as evident from Figs. 12 and 13 showing the measured and modeled Q and L_{eff} of a 2 turn planar spiral inductor with 7.2 mils distance above the ground plane. The values of $L, R_s, R_,$p and C for each inductor shown in Table I are optimized to match the measured Q and the L_{eff} and their values are summarized in Table II.

TABLE II
SUMMARY OF LUMPED ELEMENT VALUES USED IN THE LTCC INDUCTOR MODEL

Type	# of turns	H (mils)	L (nH)	Rs(Ω)	Rp(kΩ)	C(pF)
2D (planar)	2	7.2	4.1	0.55	6	0.7
2D	2	14.4	5.1	0.55	6.2	0.47
2D	2	21.6	5.7	0.55	10	0.4
2D	3	7.2	8.5	0.75	5	1.3
2D	3	14.4	11.2	0.75	6.5	0.9
2D	3	21.6	13	0.75	9	0.75
3D	2	7.2	6	0.7	6	0.9
3D	2	14.4	7.5	0.7	9	0.65
3D	2	21.6	8.4	0.7	12	0.57

An evolution of the conventional 3-D type proposed to improve the SRF is shown in Fig. 14 [3]. This helical type of inductor has half a turn on each layer, and thereby increases the distance between a half turn and the underlying turns. Such configuration is useful to alleviate the capacitive coupling problem arising in the conventional type in Fig. 4, and thus, potentially prevents significant degradation in SRF. Such configuration has been fabricated and characterized with

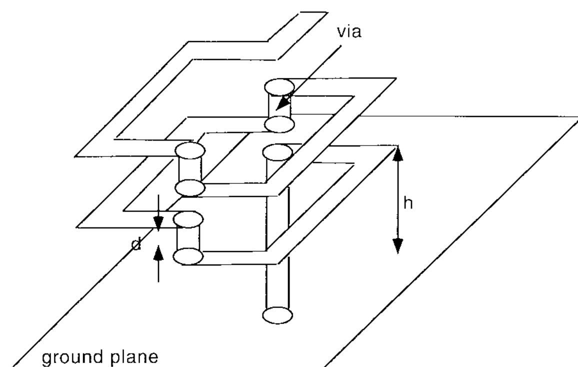

Fig. 14. Schematic diagram of a helical inductor structure. This architecture is potentially better than the conventional 3-D inductor.

different permutations in terms of turn shapes and vertical gap between turns [15].

III. Conclusion

We demonstrate the feasibility of using LTCC as a cost-effective, high density RF/microwave packaging solution with multilayer interconnects and embedded passives. The extracted material dielectric constant is uniform and the total loss is reasonably low to 10 GHz. Conventional planar spiral inductors, while showing high Q for small number of turns, occupy large area, and their Q and SRF degrade significantly as the number of turns increases. Experimental results and comparison study for the first time show that the multilayer inductor architecture is capable of implementing compact and high Q inductors suitable for hybrid RF/microwave system implementation.

References

[1] R. L. Brown and P. W. Polinski, "The integration of passive components into MCM's using advanced low-temperature cofired ceramics," *Int. J. Microcirc. Electron. Packag.*, vol. 16, no. 4, pp. 328–338, 1993.
[2] K. H. Drue, H. Thust, and J. Muller, "RF models of passive LTCC components in the lower Gigahertz-range," *Appl. Microw. Wireless*, pp. 26–35, Mar. 1998.
[3] D. L. Wilcox, R. F. Huang, and D. Anderson, "The multilayer ceramic integrated circuit (MCIC) technology: Opportunities and challenges," in *Proc. Int. Symp. Microelectron.*, 1997, pp. 17–23.
[4] W. Eurskens, *et al.*, "Design and performance of UHF band inductors, capacitors and resonators using LTCC technology for mobile communication systems," in *Proc. IEEE Int. Microwave Symp.*, vol. 3, pp. 1285–1288, 1998.
[5] A. Fathy *et al.*, "Design of embedded passive components in low-temperature cofired ceramic on metal (LTCC-M) technology," in *Proc. IEEE Int. Microwave Symp.*, 1998, vol. 3, pp. 1281–1284.
[6] R. B. Marks, "A multiline method of network analyzer calibration," *IEEE Trans. Microwave Theory Tech.*, vol. 39, pp. 1205–1215, July 1991.
[7] C. A. Hoer, "Choosing line lengths for calibrating network analyzers," *IEEE Trans. Microwave Theory Tech.*, vol. 43, pp. 76–78, Jan. 1995.
[8] "Applying the HP8510B TRL Calibration for Non-Coaxial Measurements," Product Note 8510-8, Hewlett Packard Co., Oct. 1987.
[9] R. E. Collin, *Foundations for Microwave Engineering.* New York: McGraw-Hill, 1992, ch. 3, pp. 175–176.
[10] D. I. Amey, S. J. Horowitz, and R. L. Keusseyan, "High frequency electrical characterization of electronic packaging materials: Environmental and process considerations," in *Proc. 4th Int. Symp. Exh. Adv. Packag. Mater.*, Mar. 1998, pp. 123–128.
[11] S. Mehmet, *et al.*, "A 2.4 GHz bipolar oscillator with integrated resonator," *IEEE J. Solid-State Circuits*, pp. 268–270, Feb. 1996.
[12] H. Okabe, *et al.*, "Characterization of spiral inductor on a composite-resin low-impedance substrate and its application to microwave circuits," *IEEE Trans Comp., Packag., Manufact. Technol. B*, vol. 21, pp. 269–273, Aug. 1998.
[13] A. Sutono, A. Pham, J. Laskar, and W. R. Smith, "Investigations of multilayer ceramic-based MCM technology," in *Proc. Elect. Perf. Electron. Packag.*, 1998, pp. 83–86.
[14] T. Itoh, "Overview of quasiplanar transmission lines," *IEEE Trans. Microwave Theory Tech.*, vol. 37, pp. 275–280, Feb. 1989.
[15] A. Sutono, A. Pham, J. Laskar, and W. R. Smith, "Development of three dimensional ceramic-based MCM inductors for hybrid RF/microwave applications," in *Proc. RFIC Symp.*, Anaheim, CA, 1999.

Albert Sutono received the B.S. degree from electrical engineering from Iowa State University, Ames, in 1996 and is currently pursuing the M.S. degree at the Georgia Institute of Technology, Atlanta.

In 1997, he joined Microwave Applications Group, Georgia Institute of Technology, where he has been working primarily on bond wire and organic high density interconnects for microwave packaging and embedded passive design. His current research interest is the development of integral passives on multichip-module for RF/Microwave system on package applications.

Anh-Vu H. Pham (M'99) received the B.E.E. (with highest honors), M.S., and Ph.D. degrees in electrical engineering from the Georgia Institute of Technology, Atlanta, in 1995, 1997, and 1999, respectively.

In 1997, he co-founded RF Solutions, a high-tech RF IC company, and became a Senior Member of Technical Staff. He has been an Assistant Professor with the Department of Electrical and Computer Engineering, Clemson University, Clemson, SC, since 1999. He has published over 15 journal and conference papers related to high-frequency applications. His current research interests include microwave/millimeter wave electronics packaging and subsystem/MMIC designs.

Dr. Pham is a member of Tau Beta Pi and the IEEE MTT-12b Microwave and Millimeter Wave Manufacturing.

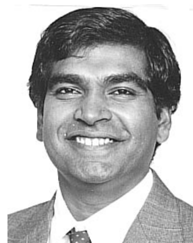

Joy Laskar received the B.S. degree (with highest honors) in computer engineering from Clemson University, Clemson, SC, in 1985 and the M.S. and the Ph.D. degrees in electrical engineering from the University of Illinois at Urbana-Champaign, in 1989 and 1991, respectively.

From 1986 to 1987, he was a Staff Engineer at IBM's T. J. Watson Research Center, Yorktown Heights, NY. From 1991 to 1992, he served as Visiting Assistant Professor at the University of Illinois at Urbana-Champaign. From 1992 to 1994, he served as Assistant Professor at the University of Hawaii at Manoa. From 1995 to 1998, he was an Assitant Professor in the School of Electrical and Computer Engineering, Georgia Institute of Technology (Georgia Tech), Atlanta. Since 1998, he has been an Associate Professor in the School of Electrical and Computer Engineering, Georgia Tech. His research has focused on wide bandwidth on-wafer characterization and design techniques through 110 GHz with applications to monolithic microwave integrated circuits (MMIC's) and high speed packages. He heads a research group of 20 members with a foucs on integration of high frequency electronics with optoelectronics and integration of mixed technologies for next generation wireless systems. He has published over 40 peer reviewed articles in IEEE and APS journals and presented over 50 conference papers.

Dr. Laskar received the Army Research Office's Young Investigator Award in 1995 and the National Science Foundation's CAREER Award in 1996. He is a co-organizer and Chair for the Advanced Heterostructure Workshop, serves on the IEEE Microwave Theory and Techniques Symposia Technical Program Committee, and is member of the North American Manufacturing Initiative roadmapping committee.

William R. Smith, photograph and biography not available at the time of publication.